# OPTICAL FIBER MANUFACTURING TECHNIQUES

**Donald P. Jablonowski, Un Chul Paek, and Laurence S. Watkins**



***Donald P. Jablonowski*** *is with AT&T Network Systems in Atlanta.* ***Un Chul Paek*** *and* ***Laurence S. Watkins*** *are with the AT&T Engineering Research Center, Princeton, New Jersey. Mr. Jablonowski is department chief, Preform and Draw Process Development. In his department, fabrication techniques for advanced optical fibers are perfected. He received a B.S., M.S., and Ph.D. in electrical engineering from Carnegie-Mellon University. He joined AT&T in 1973. Mr. Paek is a consulting member of the technical staff and a Fellow of AT&T Bell Laboratories. He has specialized in the areas of fiber drawing and coating, fiber strength, and light propagation in fibers. He received a B.S. degree from Korea Merchant Marine Academy and M.S. and Ph.D. degrees in mechanical engineer-*
(continued on page 44)

The cost of fiber has been steadily decreasing because of the experience learned in production and developments in fiber processing. In this paper we will review the processes for making optical fibers, dwelling mostly on the fiber drawing process. Our results show that the fiber draw rate has been increased to more than 10 m/s without any degradation in fiber performance and specifications. The technology is not fully mature and it is likely that even higher rates should be achievable.

## Introduction

The cost of fiber has been steadily decreasing since large-scale production was started in 1979. This has been due to both the experience learned in production and a series of major developments in fiber processing and the associated equipment. There is no doubt that this trend will continue for some time, resulting in continued reduction in the cost of fiber. Coupled with this trend has been the continuing demand to maintain and improve the performance specifications of the fiber.

In optical fiber technology there have been significant developments to increase the production rate. The shape and size of preforms depend to some extent on the fabrication technique; current diameters can range between 1 and 2 cm. Further efforts to scale up the preform process are likely to result in diameters in excess of 2 cm.

Since most of the glass in the preform is cladding, current developments are focusing on techniques to produce cladding glass as fast as possible. Parallel developments are required in fiber drawing technologies which will require larger furnaces to accommodate the larger diameter preforms and higher draw speeds to process massive amounts of glass.

In this paper we will review the processes to make optical fibers, dwelling on the fiber drawing process. The modified chemical vapor deposition (MCVD) process to make preforms is briefly described below; a more extensive article dealing with this process may be found in Reference 1.

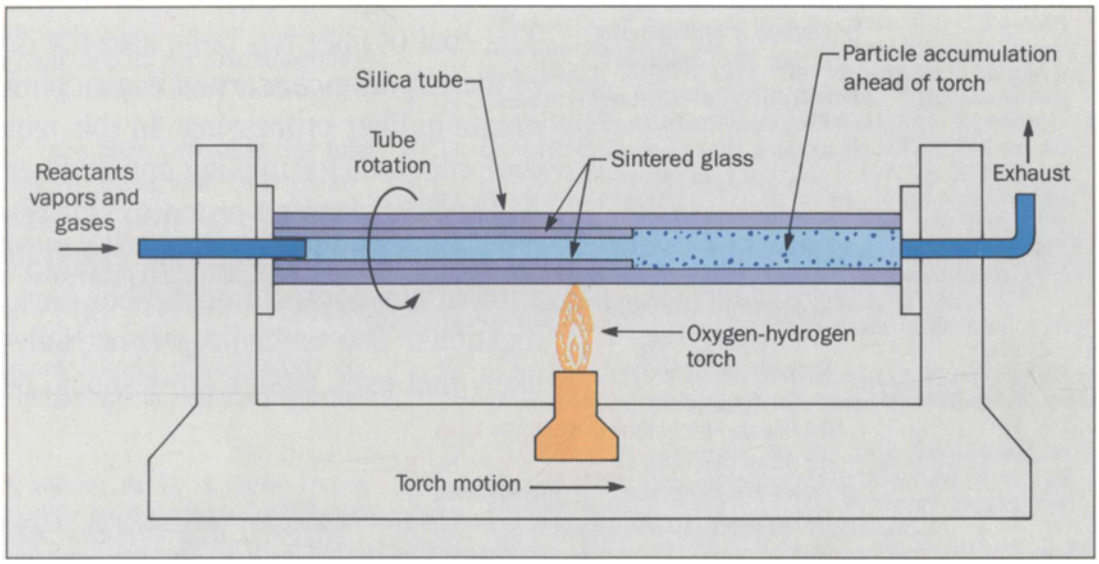


**Figure 1. Schematic of the modified chemical vapor deposition process.**



### The MCVD Process

The MCVD process (Figure 1) was invented at AT&T Bell Laboratories in the early 1970s.[1-3] High-purity dry vapor of $SiCl_4$ with various combinations of vapors of $GeCl_4$ and fluorinated hydrocarbons are passed through a rotating silica substrate tube along with pure oxygen. An external oxyhydrogen torch heats the tube and the contents react to form silica glass particles doped with the desired combinations of germanium and fluorine. Downstream from the reaction the particles are driven to the tube walls by thermophoretic forces, where they deposit. The moving torch that first caused the reaction to occur then passes over this deposit and sinters it into a thin layer of doped glass. A number of layers are deposited by repeated passes of the torch. The relative proportion of the vapors is adjusted at each pass to provide the desired composition profile and so give the fiber its index profile.

The next step involves heating the quartz tube to a high temperature by slowly moving the same oxyhydrogen torch along the length of the tube. At a high enough temperature, the glass approaches its softening point, and surface tension causes the tube with the deposited glass layers to collapse uniformly into a solid rod called a preform.

The AT&T manufacturing facility was started up in Atlanta in 1979, and by the end of 1986, over 1.7 Mkm of fiber in lightguide cable had been shipped. The MCVD process is exceptionally well-suited for producing high-performance single-mode fibers of various designs. The layer structure and the ability to incorporate a variety of dopants at various concentrations makes it convenient to fabricate designs of any complexity. In addition, the manufacturing equipment is readily adjusted through software modifications to produce any design. Finally, the process is inherently reproducible and leads to tight distributions of fiber properties.[1]

Subsequent to the MCVD process, the preform is inserted into a high-temperature furnace and a fiber is drawn. The standard outside diameter is 125 μm. An in-line operation adds a 60-μm-thick polymer coating to the

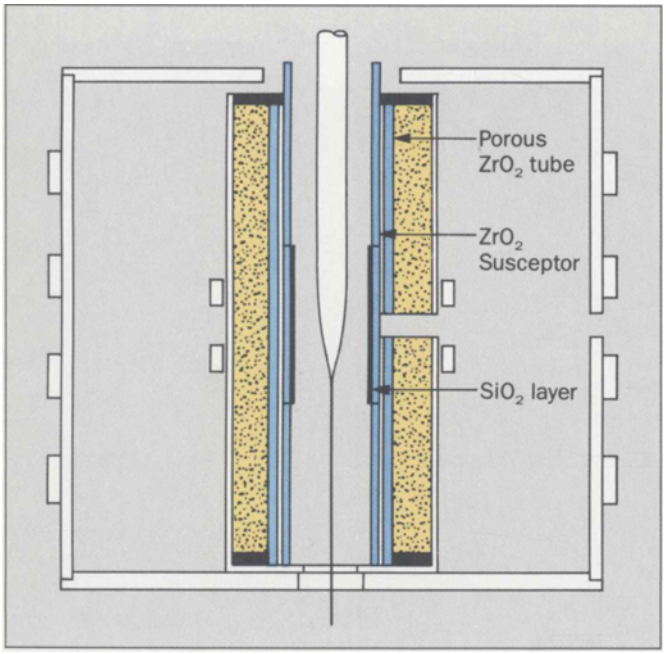


**Figure 2. Configuration of the new zirconia induction furnace. The middle piece of the inner tube (susceptor) that is loosely sleeved with a low-density zirconia tube is covered with a thin glassy film.**

fiber in order to protect the glass surface from damage. The physical properties of the coating are selected to enhance subsequent cabling and splicing operations and to mitigate microbending deformations that could lead to optical loss. The entire fiber length is tested for strength (proof tested), typically at 50 ksi. The proof test guarantees a minimum level of mechanical integrity for subsequent cabling, installation, and service operations. The local strength in a short length (a few centimeters) is much higher than the proof test level, typically 800 ksi, and this serves to make the fiber easy to handle, for example, in splicing operations. A detailed discussion of the drawing process is presented in the next section.

### The Fiber Drawing Process

The fiber drawing process has seen significant developments in recent years. Not only the drawing speed but also furnace size is increasing as larger diameter preforms are being made. At the same time, diligence is required to design furnaces to ensure that they are not sources of particle contamination which will degrade fiber strength.

Coating speeds are already in the 5-m/s range in production and up to 20-m/s speeds have been published in research work.[4] This also requires advances in furnace design to ensure the correct draw tension, fiber cooling techniques, and application developments to properly apply multilayer protective coatings. Finally, it requires dimensional measurement and control systems to produce fiber and coating geometries within very tight specifications.

**Zirconia Draw Furnace.** Ultra-pure zirconia, fully stabilized with yttria, has desirable properties for use as a high-temperature furnace.[5] In operation, however, the zirconia susceptor tube develops cracks that can introduce zirconia particles into the heat zone via two routes: (1) particles that break off the cracked susceptor and (2) particles from the insulating grog that migrate through the cracks. A new furnace (Figure 2) was designed to prevent these particles from depositing on the preform surface.[6]

During operation of a furnace, the cracks are usually initiated in the midsection of the susceptor tube where the temperature is the highest. These cracks gradually increase in size during the life of the furnace. Finally, the tube reaches such an aggravated condition that the radio-frequency field is no longer able to couple to the fractured tube and the furnace has to be rebuilt.

**Double jacket.** To prevent zirconia particles migrating through the cracks, the susceptor tube is loosely jacketed with a low-density zirconia tube. This outer tube, because of its low density, permits the RF field to be transmitted through and be absorbed by the dense inner

susceptor tube. The absorbed energy will be converted to radiant energy that heats the preform placed inside the tube. Furthermore, the outer tube is allowed to freely expand to a certain extent and maintain a crack-free condition. Therefore the zirconia insulating grain surrounding the outer tube will be completely isolated from the inner tube and is prevented from migrating into the inside of the furnace.

**Silica layer.** The second feature of the furnace is a silica glass film which is deposited on the inner surface of the susceptor tube. To do this the middle section of the susceptor tube is mounted in the head stock of a glass lathe. A silica ring torch is placed in front of the tube. The torch is connected to a chemical delivery system to generate silica soot particles which deposit to form a uniform layer on the inside of the tube as it rotates. The thickness of the layer is between 0.5 and 1 mm (Figure 3). The susceptor is replaced in the furnace and this layer will be sintered into a glassy film as it is raised to its operating temperature.



After 3 months' operation, a sample piece was taken from the middle ring to examine the condition of this silica film with a scanning electron microscope (SEM). Figure 4a is the SEM picture of the sample showing a silica glass film about 50 μm thick resulting from the deposited soot layer.

Figure 4b is a silica map of Figure 4a showing the silica particles throughout the cross-section of the sample. The white dots represent the silica distribution, and the number of dots at a given area correspond to the silica concentration at that point. This figure clearly shows that the silica particles diffused into the zirconia substrate during the sintering process and possibly lodged in the grain boundaries of the zirconia crystals or filled in the minute voids existing between the crystals. Particularly, it is important to note that the cracks in the tube were filled with silica glass and stayed intact without noticeable progression of deterioration.

**High-Speed Drawing.** During drawing the fiber is

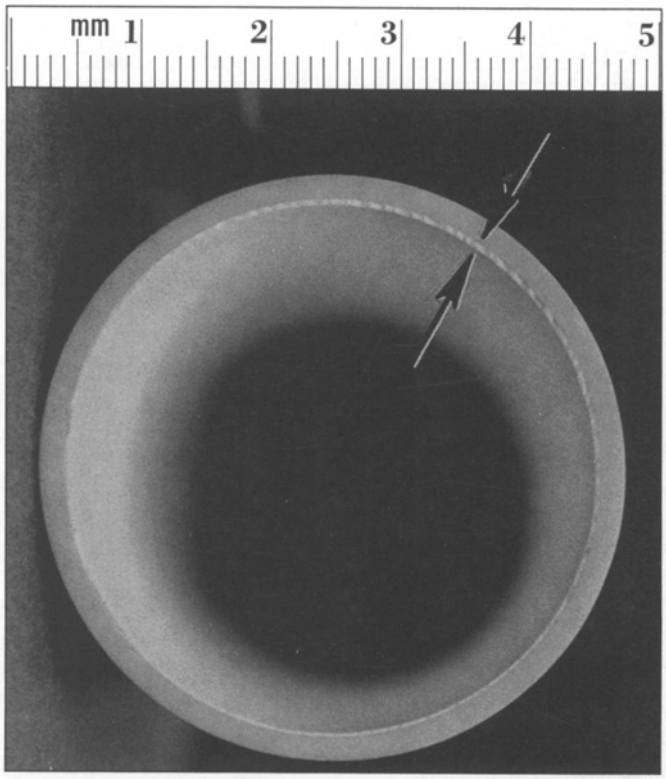


**Figure 3. Cross-sectional view of deposited soot layer inside the zirconia ring. The thickness of the layer is approximately 0.7 mm.**

continuously cooled by the surrounding air as it moves away from the furnace, but if the draw speed is increased this raises the temperature at the coating cup. Above a certain point the coating material adjacent to the fiber will be excessively heated and finally reach a temperature at which the meniscus formation no longer occurs. This meniscus collapse inhibits wetting of the coating material, resulting in incomplete coating.

To avoid excessive heating at high draw speed,

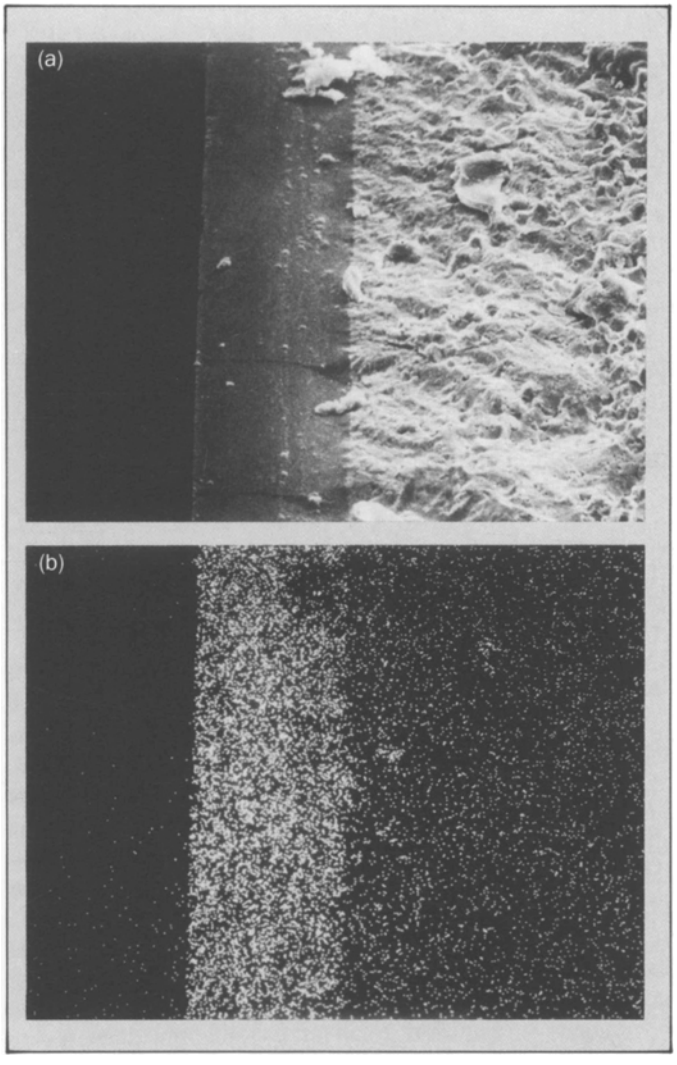


**Figure 4. (a) SEM micrograph showing the sintered silica glass film on the zirconia substrate. (b) Silica map showing silica particle density distribution across the section.**

two preventive measures can be taken: forced cooling[7] of the fiber by means of a gas and/or increasing the distance between the furnace and the coating applicator.[8] The relation between the distance $H$, measured from the bottom of the furnace to the coating cup, and draw speed $V$ is given by

$$H = \frac{\rho C_p d\theta}{4h} V \tag{1}$$

where $\rho$ is density of fiber material, $C_p$ its specific heat, $d$ fiber diameter, and $h$ the heat transfer coefficient. $\theta$ in the above expression is a dimensionless temperature which is defined by

$$\theta = \ln\left[\frac{T_s - T_o}{T_c - T_o}\right] \tag{2}$$

where $T_s$ is the lower softening point of silica, $T_o$ ambient temperature, and $T_c$ the fiber temperature at the coating cup.

Even in the case when a chiller is used for cooling the fiber, the above expression can predict the fiber temperature from the chiller on down. When the temperatures at the entrance and the exit of the chiller are $T_1$, $T_2$ respectively for a length $L$, the following expression can be obtained:

$$\frac{T_2 - T_o}{T_1 - T_o} = \exp\left[-\frac{4htL}{\rho C p d V}\right] \tag{3}$$

where $h_t$ = heat transfer coefficient within the chiller.

**High-Speed Coating.** The purpose of applying a coating is to protect the surface from external damage and preserve the original strength. The theoretical strength of silica fiber is approximately 7 GN/m$^2$ ($1 \times 10^6$ lb/ft$^2$) in air.

However, one of its shortcomings is that it can be easily damaged on its surface in contact with foreign particles or matter. Thus proper application of a thin coating on the fiber surface is needed.

Coating materials to be used for fibers can be categorized into two groups: organic material, for example ultraviolet-curable material,[9-12] thermally curable resin,[10,11] and hot melt coating,[12,13] and inorganic material such as metallic coating[14-15] and silicon nitride.[16] To assure good performance of a coated fiber, the physical properties of the candidate materials must meet stringent requirements for the physical properties of the coating.[17] In practice, ultraviolet or thermally curable materials are commonly used.

There are two types of coating application techniques that are commonly practiced in fiber manufacture. The first one is open-cup type application in which no external pressure is applied to the system. Therefore the only force existing in the applicator is the drag force from the fiber passing through the viscous material. In this case the coating thickness $t$ can be predicted by

$$t = \sqrt{\frac{(R^2 - a^2)}{2\ln(R/a)}} - a \qquad (4)$$

where $a$ is the fiber radius and $R$ is the applicator radius. Ths relation shows the important fact that the coating thickness is independent of coating speed when an unpressurized applicator is used, and is determined only by the die size and fiber diameter.

In high-speed coating, minimum shear stresses should be induced in the coating applicator. Otherwise, high shear flow may inhibit wetting if the coating material on the fiber surface or the non-Newtonian flow effect causes beading of the coating. Also, above a certain speed with an open cup, the fiber starts to slip because adhesion of the coating material at the fiber interface cannot sustain the drag force. To prevent this slippage, a mechanism that will provide a reduction of relative velocity between the fiber and the fluid in the cup must be introduced. The pressurized applicator[18] effectively eliminates this problem with the acceleration of fluid motion by the external pressure.

Pressure coating application is now the most prevalent technique in high-speed coating. The coating thickness is found to follow a linear relationship with a dimensionless quantity $S$, for a given fiber diameter and die size:

$$t = A \cdot S + B \qquad (5)$$

In the above expression, $A$ and $B$ are constants depending on $a$ and $R$. The dimensionless quantity $S$ is defined by

$$S = \frac{\Delta p R^2}{8\eta VL} \qquad (6)$$

where $\Delta p$ is the pressure differential applied to the applicator, $\eta$ the material viscosity, and $L$ the applicator land length.

Therefore, Equation (5) shows the functional dependence of the various process parameters as well as system parameters. For instance, the thickness increases linearly with increasing pressure but depends inversely on the draw speed $V$ and the viscosity $\eta$. A more explicit description of the thickness variation and draw speed can be found in Figure 5.[19] The viscosity of polymer material responds sensitively to temperature $T$, and decreases exponentially with increasing temperature.[20] Thus, in pressurized coating the heating effect of coating material in a coating cup is equivalent to an increase in pressure because the dimensionless pressure $S$ is increased by decreasing the viscosity, therefore resulting in an increase in the coating thickness.

**Strength of High-Speed-Coated Fiber.** One of the noticeable differences in high-speed coating is the draw

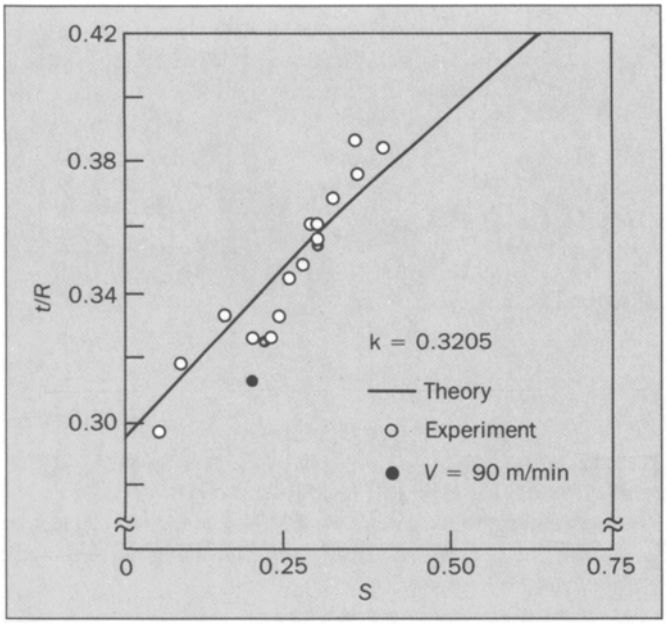


**Figure 5. Relation between normalized coating thickness and dimensionless quantity S for a pressurized coating applicator; $k = a/R$ (from Reference 17).**

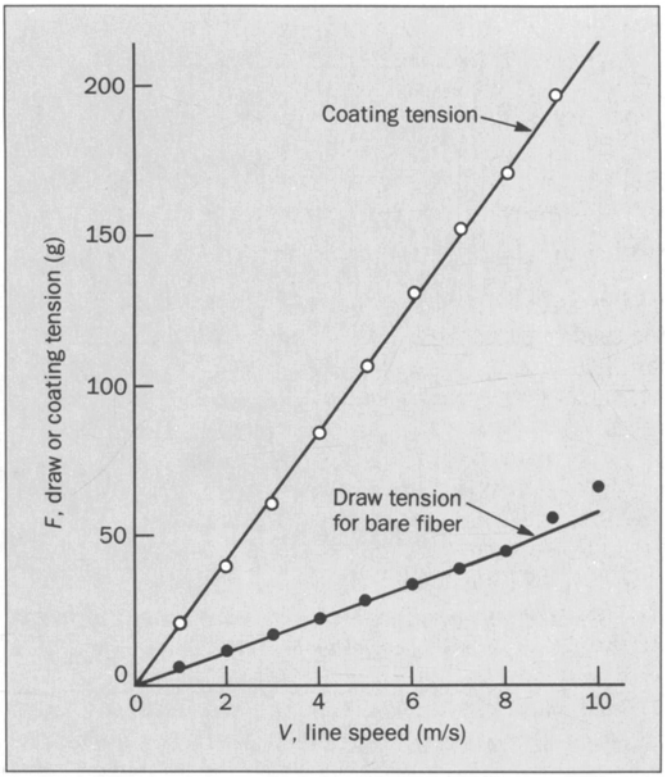


**Figure 6. Relationships of draw and coating tension to coating speed. Both increase linearly with the line speed at constant temperature.**

tension, which is maintained at a much higher level than for low speed. The important fact that has to be remembered is that the draw tension increases linearly with draw speed and will thus imbed increased residual stresses in the composite structured drawn fiber.[21] Such stresses in the fiber core will not only affect the strength characteristics but also influence the optical properties. Therefore it was important to study the effect of this high tension on the fiber transmission loss as well as on the strength.

The draw tension depends on several parameters, i.e., preform diameter, fiber diameter, furnace temperature, and draw speed.[22] We measured the draw tension for different line speeds at a fixed furnace temperature and found that the tensions with and without applying the coating are both linearly dependent on draw speed, as shown in Figure 6. This figure also shows that in the case of coating application, tension reaches about 200 g at the speed of 10 m/s, while the tension for bare fiber drawing at the same speed is about 50 g.

Another problem to note here is bubble inclusion in the coating. During coating the fiber drags air into the fluid, and these air bubbles accumulate in the coating mate-

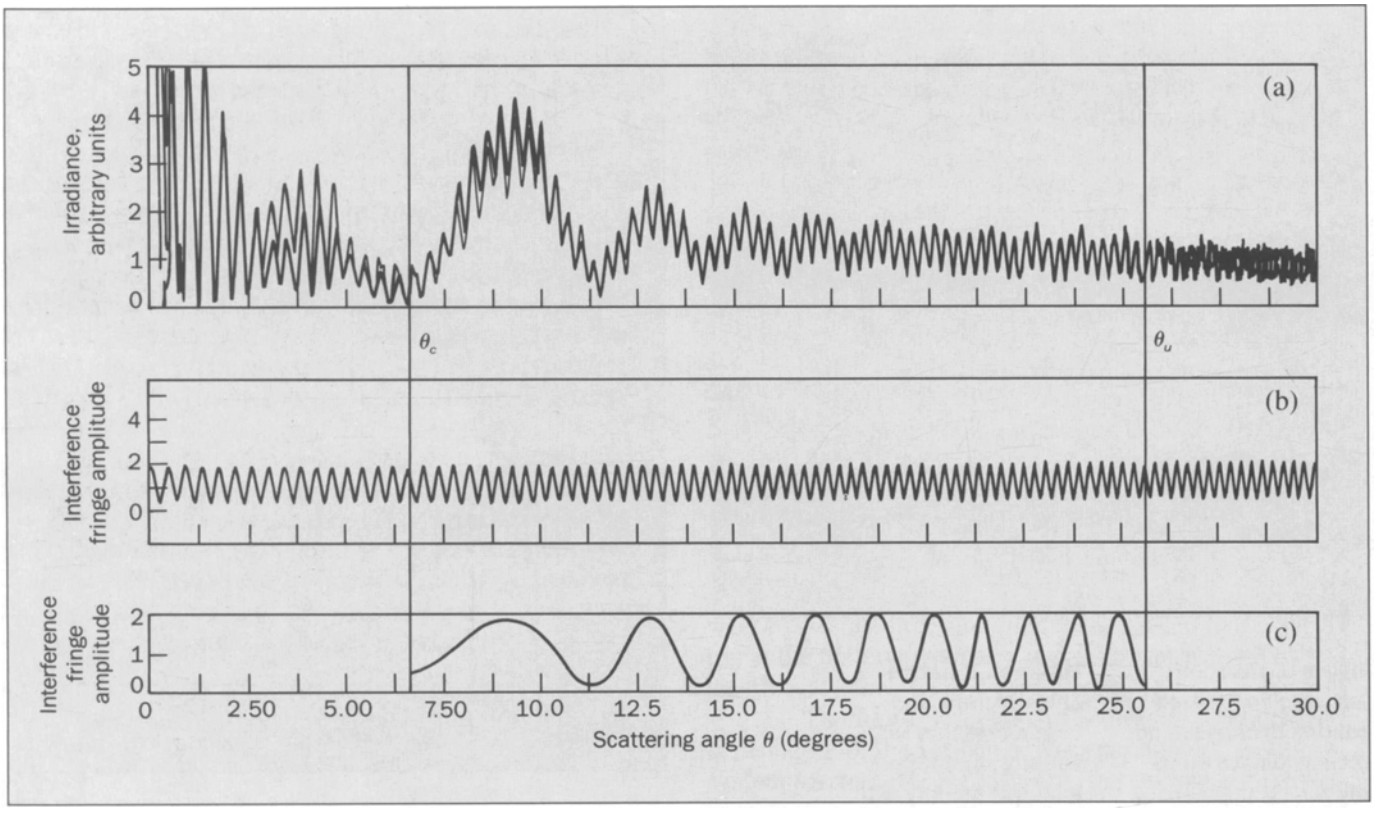


**Figure 7. Composite graph of experimental and theoretical forward-scattering patterns for a step-index fiber. (Data for angles between 30° and 80° have been omitted since there is little change in structure in this range.) (a) Comparison of wave theory to experimentally measured patterns (heavy line is experimental data.). (b) Fringe position and (c) fringe modulation calculated from geometric ray tracing. The number of fringes is proportional to the diameter.**

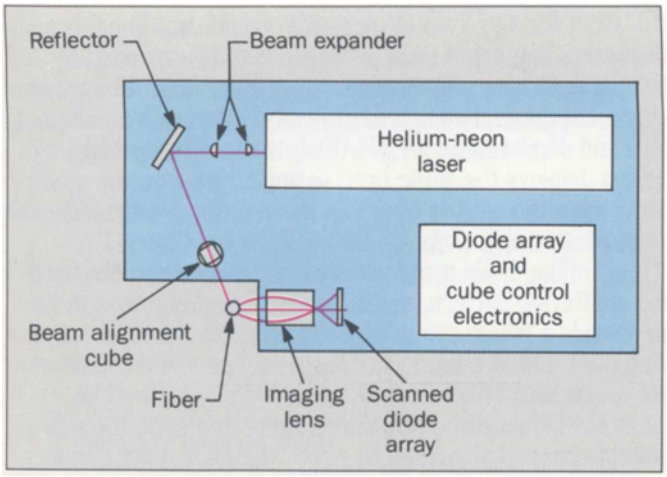


**Figure 8. Optical layout of fiber measurement apparatus. Cube rotates to center beam on the fiber.**

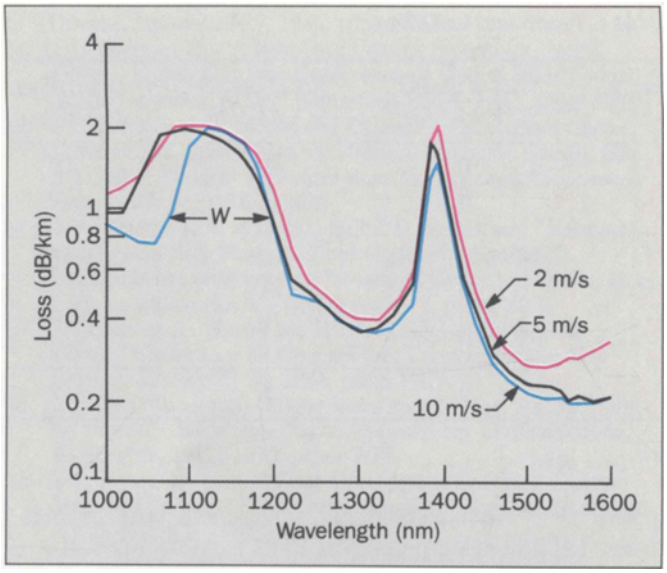


**Figure 9. Transmission losses of single-mode fibers at $\lambda$ = 1.32 $\mu$m for three different coating speeds.**



rial. These bubbles are small enough to pass through the die, and after curing, remain permanently in the coating layer. Obviously, this will lead to a problem in maintaining a good coating concentricity and ultimately result in poor fiber strength. At high speed, bubble entrainment increases significantly, and so the applicator must be designed in such a way that it prevents this.

**Control of Fiber Drawing.** The diameter of the fiber in a steady-state drawing process is governed by mass conservation. The time to attain steady state, however, can be significant, and sometimes steady state is never achieved because of local fluctuations. In addition the preform diameter may not be constant. As a consequence, there is a requirement for a diameter measurement and control system if fibers with tight dimensional tolerances are to be made.

There are a number of reasons for minimizing diameter fluctuations. In most splicing techniques,[23] the outside surface of the fiber is used as a reference when the core regions of the fiber are aligned. For single-mode fibers, the dispersion and cutoff characteristics are very sensitive to the core diameter, as well as the refractive index profile.[24,25] Variations in the fiber diameter cause the same proportional variations in the core diameter.

Between the furnace and the coating cup it is very important that the fiber not be touched or abraded, since this causes minute flaws which act as a source for crack propagation under load.[26] For similar reasons, and to minimize microbending loss[27] in the cable, it is important that the fiber be well centered in the coatings. The fact that these two measurement and control operations must be done without fiber contact led to the use of laser light scattering.

**Application of light scattering.** There have been a number of techniques developed for measuring fiber diameter by shadow techniques.[28] The most accurate method for control, however, is the forward light scattering

**Table I. Proof-Test Results**

| Sample no. | No. of breaks at 0.7 GN/m² | No. of breaks at 1.4 GN/m² | Drawn fiber length, km |
|---|---|---|---|
| 1 | 0 | 0 | 7.0 |
| 2 | 0 | 1 | 7.0 |
| 3 | 0 | 0 | 6.7 |
| 4 | 0 | 1 | 6.5 |
| 5 | 0 | 1 | 7.0 |
| 6 | 0 | 3 | 7.0 |
| 7 | 0 | 0 | 8.0 |
| | 0 | 6 | 49.2 |

NOTE: $V$ = 10 m/s.

approach.[29-32] When a collimated single-mode laser beam is directed at a fiber perpendicular to its axis, light is scattered in the plane perpendicular to the fiber axis. The light flux scattered as a function of the angle measured with respect to the forward direction of the incident beam is characteristic of the size of the fiber and the refractive index. If it is a clad fiber or has a transparent coating on it, the pattern will be modified by these structures.



Analysis and measurements of various patterns have been reported in a number of papers.[29-32] Figure 7 shows the intensity plot of the scattering pattern for a simple step index structure without plastic coating. The pattern basically consists of interference fringes of varying intensity in the angular range of approximately ± 5 to 90°. Changes in fiber diameter result in both movement of the fringes and a change in their angular frequency. The theoretical pattern in Figure 7 was obtained from calculated solutions of Maxwell's equations which predict all the characteristics of the pattern. Some of the dominant features, however, can be described using geometric ray tracing procedures and show that the number of fringes is directly proportional to the fiber diameter.[33]

**Fiber diameter measurement.** Figure 8 shows the optical layout for a system to measure and control fiber diameter. The beam from a He-Ne laser is expanded by cylindrical lenses and directed toward the fiber through an alignment cube. The light is collected by a low f/number lens and displayed on a 1024-diode array. The optical design displays the same precise angle range on the diode array even though the fiber can move around in the window.

The diode array provides a voltage-time display of the scattering pattern, and this is analyzed electronically to provide a fringe count which is proportional to fiber diameter. The system has 0.2-μm accuracy and can tolerate movement of the fiber within a 1-cm window. The diameter is measured at a 500-Hz rate and used through a suitable control algorithm to adjust the fiber draw motor velocity.[34]

**Fiber coating centering.** The same basic principles and geometric ray trace were used to analyze scattering from plastic-coated fibers.[35,36] The differences are that the coating can have either a smaller or larger refractive index than the core glass. The measurement is also different since it is concentricity rather than diameter which is of primary interest.

The effect of an eccentric fiber in the coating is to cause an eccentricity in the pattern. An automatic control system[36] measures these optical patterns, determining the eccentricity, and then adjusts the position of the coating applicator to center it to the fiber.

## Conclusions

The application of this technology has resulted in significant increases in fiber draw speed while maintaining the strength and optical properties of the fiber. Table I presents data on a strength experiment on a synthetic glass rod drawn at 10 m/s, showing six breaks for 49 km of fiber tested at 1.4 GN/m². More recent data indicate even better strength results.[37]

Figure 9 shows transmission loss data for fiber drawn and coated at various speeds. The data indicate a

slight reduction in loss at high speeds.

Our results show that the fiber draw rate has been increased to more than 10 m/s without any degradation in fiber performance and specifications and our analysis indicates even higher rates should be achievable.

**Acknowledgment**

The authors wish to express their gratitude to R. J. Klaiber for his guidance and encouragement and for his help with preparing this manuscript.

**References**

1. W. M. Flegal et al., "Making Single-Mode Preforms by the MCVD Process," *AT&T Technical Journal*, Vol. 65, Issue 1, January-February 1986, pp. 56-61.
2. J. B. MacChesney, P. B. O'Connor, and H. M. Presby, "A New Technique for the Preparation of Low Loss and Graded Index Optical Fibers," *Proceedings of IEEE*, Vol. 62, 1974, pp. 1278-1279.
3. T. Li, ed., *Optical Fiber Communications*, Vol. 1, Academic Press, New York, 1985.
4. R. B. Runk, "A Zirconia Induction Furnace for Drawing Precision Silica Waveguides," Topical Meeting on Optical Fiber Communication, Williamsburg, Virginia, 1977, paper TuB5-1.
5. S. Sakaguchi and T. Kimura, "A 1200 m/min Speed Drawing of Optical Fiber with Pressure Coating," Conference on Optical Fiber Communication, San Diego, February 11-13, 1985, paper MG2.
6. U. C. Paek and C. M. Schroeder, "Silica Coated Dual-Tube $ZrO_2$ Induction Furnace for High Strength Optical Fibre Production," *Electronics Letters*, Vol. 22, 1986, p. 72.
7. C. M. Darcangelo, M. R. Montieth, and Y. M. Ni, "Fiber Cooling Apparatus," U.S. Patent 4514205.
8. U. C. Paek and C. M. Schroeder, "High Speed Coating of Optical Fibers with UV Curable Materials at a Rate of Greater than 5 m/sec," *Applied Optics*, Vol. 20, 1985, p. 135.
9. U. C. Paek and C. M. Schroeder, "Calculation of Photopolymerization Energy Required for Optical Fiber Coating," *Applied Optics*, Vol. 20, 1981, p. 1230.
10. N. Inagaki and S. Yamakawa, "High Speed Coating and Coating Materials for Optical Fibers," Conference on Optical Fiber Communication, New Orleans, January 23-25, 1984, paper WF1.
11. S. Araki et al., "Fabrication of High Strength Long Length Fibers," Conference on Optical Fiber Communication, New Orleans, January 23-25, 1984, paper WF3.
12. L. L. Blyler et al., "A New Dual Coating System for Optical Fibers," Eighth European Conference on Optical Fiber Communication, Cannes, France, September 21-24, 1982, paper AV11.
13. T. J. Miller et al., "Silicone and Ethylene-Vinyl-Acetate Coated Laser Drawn Silica Fibers with Tensile Strengths Greater than 3.5 GN/m² (500 ksi) in Greater than 3 km Lengths," *Electronics Letters*, Vol. 14, 1978, p. 603.
14. D. A. Pinnow, J. A. Wysocki, and G. D. Robertson, "Hermetically Sealed High Strength Fiber Optical Waveguides," International Conference on Integrated Optics and Optical Fiber Communication (IOOC'77), Tokyo, 1977, paper B9-5.
15. S. Tanaka et al., "Low Loss Hermetically Coated Optical Fibers," Conference on Optical Fiber Communication, New Orleans, January 23-25, 1984, paper WF7.
16. R. Hiskes, "Improved Fatigue Resistance of High Strength Optical Fibers," Topical Meeting on Optical Fiber Communication, Washington, D.C., 1979, paper WF6.
17. L. L. Blyler, Jr., et al., "Fiber Drawing and Coating," Topical Meeting on Optical Fiber Communication, New Orleans, February 28-March 2, 1983, paper TuF1.
18. C. R. Taylor, "Fiber with Multiple Coatings," U.S. Patent 4480898.
19. A. Panoliaskos, W. L. H. Hallett, and I. Garis, "Prediction of Optical Fiber Coating Thickness," *Applied Optics*, Vol. 24, 1985, p. 2309.
20. K. Chida et al., "High Speed Coating of Optical Fibers with Thermally Curable Silicone Resin Using a Pressurized Die," *Electronics Letters*, Vol. 18, 1982, p. 713.
21. U. C. Paek and C. R. Kurkjian, "Calculation of Cooling Rate and Induced Stresses in Drawing of Optical Fibers," *Journal of the American Ceramic Society*, Vol. 58, 1975, p. 330.
22. U. C. Paek and R. B. Runk, "Physical Behavior of the Neck Down Region during Furnace Drawing of Silica Fibers," *Journal of Applied Physics*, Vol. 49, 1978, p. 4417.
23. J. F. Dalgleish, "Splices, Connectors and Power Couplers for Field and Office Use," *Proceedings of IEEE*, Vol. 68, 1980, p. 1226.
24. U. C. Paek, G. E. Peterson, and A. Carnevale, "Parametric Effects to the Bandwidth of a Single Mode Fiber with Experimental Verification," *Applied Optics*, Vol. 21, 1982, p. 704.
25. L. G. Cohen et al., "Transmission Studies of a Long Single Mode Fiber—Measurements and Considerations for Bandwidth Optimization," *Bell System Technical Journal*, Vol. 60, 1981, p. 1713.
26. L. L. Blyler, Jr., and F. V. DiMarcello, "Fiber Drawing, Coating

and Jacketing," *Proceedings of IEEE*, Vol. 68, 1980, pp. 1194-1198.
27. W. B. Gardner, "Microbending Loss in Optical Fibers," *Bell System Technical Journal*, Vol. 54, 1975, p. 457.
28. Product literature for Milmaster electronic micrometer, The Electron Machine Corp., Umatilla, Florida; Model 1160A Lasermike™ optical micrometer, Systems Research Labs, Inc., Dayton, Ohio; Anritsu M417 SLB diameter measuring system, Anritsu Electric Co. Ltd., Tokyo.
29. M. Kerker and E. Matijevic, "Scattering of Electromagnetic Waves from Concentric Infinite Cylinders," *Journal Optical Society of America*, Vol. 51, 1961, p. 506.
30. H. C. van der Hulst, *Light Scattering from Small Particles*, Wiley, New York, 1957.
31. J. L. Lundberg, "Light Scattering from Image Fibers at Normal Incidence," *Journal of Colloid and Interface Science*, Vol. 29, 1969, p. 565.
32. L. S. Watkins, "Scattering from Side-Illuminated Clad Glass Fibers for Determination of Fiber Parameters," *Journal Optical Society of America*, Vol. 65, 1974, p. 767.
33. D. H. Smithgall, L. S. Watkins, and R. E. Frazee, Jr., "High Speed Non-Contact Fiber Diameter Measurement Using Forward Light Scattering," *Applied Optics*, Vol. 16, 1977, p. 2395.
34. D. H. Smithgall, "Application of Optimization Theory to the Control of Optical Fiber Drawing Process," *Bell System Technical Journal*, Vol. 58, No. 6, July-August 1979, p. 1425.
35. B. R. Eichenbaum, "The Centering of Optical Fiber Coatings by Monitoring Forward Scattering Patterns," *Bell System Technical Journal*, Vol. 59, No. 3, March 1980, p. 313.
36. D. H. Smithgall and R. E. Frazee, Jr., "High Speed Measurement and Control of Coating Concentricity," *Bell System Technical Journal*, Vol. 60, No. 9, November 1981, p. 2065.



Biographies (continued)

*ing from the University of California, Berkeley. He joined AT&T in 1969. Mr. Watkins is supervisor of the Fiber and Integrated Optics Group. He joined AT&T in 1966, and has specialized in the development of optical measurement techniques. He received the B.S. in electronic engineering and the Ph.D. in quantum electronics, both from Southampton University, England.*

*(Manuscript received November 12, 1986)*